Host factors in the pathogenesis of HIV infection	Tatsuo Shioda	International Congress on Medical Virology 2014	2014 年 11 月	国外
TRIM5 α による HIV-1 および HIV-2 のカプシドコアの脱殻促進：可視化ウイルスによる解析	武田英里，河野健，Amy E. Hulme, Thomas J. Hope, 中山英美，塩田達雄	第 62 回日本ウイルス学会学術集会	2014 年 11 月	国内
HIV-1 パッケージングシグナル内最重要領域 SL1 の機能的構造に関する多角的解析	櫻木淳一，櫻木小百合，塩田達雄	第 62 回日本ウイルス学会学術集会	2014 年 11 月	国内
Novel mutant HIV-1 strains with high degree of resistance to cynomolgus macaque TRIMCyp generated by random mutagenesis	Tahmina Sultana, 中山英美，飛田哲志，齊藤暁，明里宏文，塩田達雄	第 28 回日本エイズ学会学術集会	2014 年 12 月	国内
TRIM5 α存在下における HIV-1 および HIV-2 のカプシドコアの脱殻	武田英里，河野健，Amy E. Hulme,Thomas J. Hope, 中山英美，塩田達雄	第 28 回日本エイズ学会学術集会	2014 年 12 月	国内
再生医療技術のエイズ研究応用のためのアカゲザル iPS 細胞樹立と CD34 陽性細胞への分化	田谷かほる，武田英里，中山英美，塩田達雄，明里宏文，金子新	第 28 回日本エイズ学会学術集会	2014 年 12 月	国内
HIV パッケージングシグナル内最重要領域 SL1 の機能的構造に関する多角的解析	櫻木小百合，塩田達雄，櫻木淳一	第 28 回日本エイズ学会学術集会	2014 年 12 月	国内
Genome-wide association study of HIV-related lipoatrophy in Thai patients: Association of a DLGAP1 polymorphism with fat loss.	中山英美，Uttayamakul Sumonmal, Tiphaine Oudot-Mellakh, Pimrapat Tengtrakulcharoen, Julien Guergnon, Jean-Francois Delfraissy, Srisin Khusmith,Chariya Sangsajja, Sirirat Likanonsakul, Ioannis Theodorou, 塩田達雄	第 28 回日本エイズ学会学術集会	2014 年 12 月	国内
Host Factors in the Pathogenesis of HIV Infection.	Tatsuo Shioda	17th International Conference on Emerging Infectious Diseases (EID) AIDS Panel Meeting	2015 年 1 月	国外
Lack of Association between Intact/Deletion Polymorphisms of the APOBEC3B Gene and HIV-1 Risk.（ポスター）	Imahashi M, Izumi T, Imamura J, Matsuoka K, Ode H, Masaoka T, Sato K, Koyanagi Y, Takaori-Kondo A, Yokomaku Y, Sugiura W, Iwatani Y.	Cold Spring Harbor Laboratory Annual meeting on Retroviruses, Cold Spring Harbor, NY, USA	2014 年 5 月	国外
Fine-tuned HIV-1 Vif- interaction interface of anti-retroviral cytidine deaminase APOBEC3F.（ポスター）	Nakashima M, Kitamura S, Kurosawa T, Ode H, Kawamura T, Mano Y, Naganawa Y, Yokomaku Y, Watanabe N, Sugiura W, Iwatani Y	Cold Spring Harbor Laboratory Annual meeting on Retroviruses, Cold Spring Harbor, NY, USA	2014 年 5 月	国外
23rd Congress and general assembly of the international union of crystallography（ポスター）	Nakashima M, Kitamura S, Kurosawa T, Ode H, Kawamura T, Imahashi Y, Yokomaku Y, Watanabe N, Sugiura W, and Iwatani Y	23rd Congress and general assembly of the international union of crystallography, Montreal, Canada	2014 年 8 月	国外
HIV-1 感染急性期における HIV 特異的な病態バイオマーカーの探索について（ポスター）	重見麗，蜂谷敦子，松田昌和，今村淳治，渡邊綱正，横幕能行，岩谷靖雅，杉浦亙	第 28 回日本エイズ学会学術集会	2014 年 12 月	国内
HIV-1 Vif における APOBEC3C/F 結合インターフェース（口頭発表）	大出裕高，中島雅晶，河村高志，北村紳悟，長縄由里子，黒澤哲平，真野由有，粟津宏昭，松岡和弘，横幕能行，渡邉信久，杉浦亙，岩谷靖雅	第 28 回日本エイズ学会学術集会	2014 年 12 月	国内
Illumina MiSeq を用いた HIV-1 近全長遺伝子配列解析の試み	松田昌和，大出裕高，松岡和弘，蜂谷敦子，横幕能行，岩谷靖雅，杉浦亙	第 28 回日本エイズ学会学術集会	2014 年 12 月	国内
Mutational Analysis of HIV-2 Vpx concerning on ability to degrade SAMHD1（口頭発表）	Ciftci Ibrahim, 藤野悠那，山本充奈美，川村宗吾，岩谷靖雅，大塚雅巳，藤田美歌子	第 28 回日本エイズ学会学術集会	2014 年 12 月	国内
Maraviroc 治療失敗症例にみる envelope 領域の遺伝的多様性の解析（口頭発表）	鬼頭優美子，大出裕高，松田昌和，松岡和弘，蜂谷敦子，清水宣明，今村淳二，岩谷靖雅，杉浦亙，横幕能行	第 28 回日本エイズ学会学術集会	2014 年 12 月	国内

HIV-1 Vif は複数の APOBEC3 結合インターフェイスをもつ（ポスター発表）	中島雅晶，大出裕高，長縄由理子，黒澤哲平，真野由有，横幕能行，杉浦亙，渡邉信久，岩谷靖雅	第 37 回日本分子生物学会年会	2014 年 11 月	国内
APOBEC3H ハプロタイプと HIV-1 感染および AIDS 発症との関連（口頭発表）	櫻井大祐，今橋真弓，岩谷靖雅，大谷仁志，成瀬妙子，照沼裕，杉浦亙，木村彰方	第 59 回日本人類遺伝学会	2014 年 11 月	国内
Deep sequencing による HIV-1 臨床検体の近全長ゲノム配列解析系の構築（口頭発表）	大出裕高，松岡和弘，松田昌和，蜂谷敦子，横幕能行，岩谷靖雅，杉浦亙	第 62 回日本ウイルス学会学術集会	2014 年 11 月	国内
空間的に異なる APOBEC3 結合インターフェースをもつ（口頭発表）	中島雅晶，大出裕高，河村高志，北村紳悟，長縄由里子，黒澤哲平，真野由有，粟津宏昭，松岡和弘，横幕能行，渡邉信久，杉浦亙，岩谷靖雅	第 62 回日本ウイルス学会学術集会	2014 年 11 月	国内
新規エントリー阻害剤の組み合わせによる抗ウイルス効果と耐性変異の解析（口頭）	原田恵嘉、横山勝、Samatchaya Boonchawalit、佐藤裕徳、松下修三、吉村和久．	第 16 回白馬シンポジウム	2014 年 6 月	国内
Impact of Maraviroc (MVC)-resistant mutations in C1 and C4 regions of gp120 on sensitivity to antibody-mediated neutralization（ポスター）	Samatchaya Boonchawalit, Shigeyoshi Harada, Shuzo Matsushita, Kazuhisa Yoshimura.	20th International AIDS Conference	2014 年 7 月	国外
Impact of Maraviroc (MVC)-resistant mutations in C1 and C4 regions of gp121 on sensitivity to antibody-mediated neutralization（口頭）	Samatchaya Boonchawalit, Shigeyoshi Harada, Shuzo Matsushita, Kazuhisa Yoshimura.	15th Kumamoto AIDS Seminar	2014 年 10 月	国外
Resistance Profile of CD4 Mimic Small Compounds (CD4MCs) and the Structure Analysis by Molecular Dynamic (MD) Simulation.（口頭）	Shigeyoshi Harada, Masaru Yokoyama, Samatchaya Boonchawalit, Hironori Sato, Shuzo Matsushita, Kazuhisa Yoshimura.	15th Kumamoto AIDS Seminar	2014 年 10 月	国外
Resistance Profile of CD4 Mimic Small Compounds (CD4MCs) and the Structure Analysis by Molecular Dynamic (MD) Simulation.（ポスター）	Shigeyoshi Harada, Masaru Yokoyama, Samatchaya Boonchawalit, Hironori Sato, Shuzo Matsushita, Kazuhisa Yoshimura.	HIV Research For Prevention	2014 年 10 月	国外
CD4 類似低分子化合物誘導体 (CD4MCs) の耐性プロファイルと分子動力学的機構解析（口頭）	原田恵嘉、横山勝、Samatchaya Boonchawalit、佐藤裕徳、松下修三、吉村和久．	第 62 回日本ウイルス学会学術集会	2014 年 11 月	国内
Impact of maraviroc (MVC)-resistant mutations in the C1 and C4 regions of gp120 on sensitivity to antibody-mediated neutralization（口頭）	Samatchaya Boonchawalit、原田恵嘉、 松下修三、吉村和久．	第 28 回エイズ学会学術集会	2014 年 12 月	国内
HIV 感染者唾液を用いたに口腔疾患発症予測因子の検討（口頭）	泉福英信、有家巧、富永燦、丸岡豊、 吉村和久．	第 28 回エイズ学会学術集会	2014 年 12 月	国内
代表的な薬剤耐性のメカニズム（口頭）	吉村和久	第 28 回エイズ学会学術集会	2014 年 12 月	国内
Impact of the Drug-Escaped HIV Envelope Mutations on Susceptibility to Neutralizing Antibodies.（口頭）	Kazuhisa Yoshimura	17th International Conference on Emerging Infectious Diseases (EID), AIDS Panel Meeting	2015 年 1 月	国外
Mutations at the bottom of the Phe43 cavity are responsible for cross-resistance to NBD analogues.（ポスター）	Shigeyoshi Harada, Yu Irahara, Samatchaya Boonchawalit,Mai Goryo, Hirokazu Tamamura, Tetsuro Matano, Shuzo Matsushita, Kazuhisa Yoshimura	The annual Conference on Retroviruses and Opportunistic Infections (CROI) 2015	2015 年 2 月	国外
クロマチン高次構造制御分子 CTCF による HTLV-I プロウイルス制御機構（口頭）	佐藤賢文、宮里パオラ、福田麻美、野坂生郷、石原宏、中尾光善、Charles Bangham：	第 1 回日本 HTLV-1 学会学術集会	2014 年 8 月	国内
クロマチン高次構造制御分子 CTCF による HTLV-I プロウイルス制御機構（口頭）	佐藤賢文、石原宏、野坂生郷、宮里パオラ、渡邊武久、中尾光善、Charles Bangham	日本血液学会学術集会	2014 年 11 月	国内

2．学会誌・雑誌等における論文掲載

TCF1 and LEF1 act as T-cell intrinsic HTLV-1 antagonists by targeting Tax	Ma G, Yasunaga J-i, Akari H, Matsuoka M	Proc Natl Acad Sci USA	2015 年 2 月	国外
New type of Sendai virus vector provides transgene-free iPS cells derived from chimpanzee blood	Fujie Y, Fusaki N, Katayama T, Hamasaki M, Soejima Y, Soga M, Ban H, Hasegawa M, Yamashita S, Kimura S, Suzuki S, Matsuzawa T, Akari H, Era T	PLoS One	2014 年 12 月	国外
Identification of SIV Nef CD8+ T cell epitopes restricted by a MHC class I haplotype associated with lower viral loads in a macaque AIDS model	Takushi Nomura, Hiroyuki Yamamoto, Naofumi Takahashi, Taeko K Naruse, Akinori Kimura, and Tetsuro Matano	Biochem Biophys Res Commun	2014 年 7 月	国外
HIV-1 Vpr induces interferon-stimulated genes in human monocyte-derived macrophages	Zahoor M A, Xue G, Sato H, Murakami T,Takeshima S-n, Aida Y	PloS ONE	2014 年 8 月	国外
Crystal structure of human importin- α 1 (Rch1), revealing a potential autoinhibition mode involving homodimerization	Miyatake H, Sanjoh A, Unzai S, Matsuda G, Tatsumi Y, Miyamoto Y, Dohmae N, Aida Y	PloS ONE	2015 年 2 月	国外
Synthesis of a Vpr-binding derivative for use as a novel HIV-1 inhibitor	Hagiwara K, Ishii H, Murakami T, Takeshima S-n, Chutiwitoonchai N, Kondo Y, Honda K, Osada H, Tsunetsugu-Yokota Y, Suzuki M, Aida Y	Antiviral Research	印刷中	国外
A high excision potential of TALENs for integrated DNA of HIV-based lentiviral vector	Ebina H, Kanemura Y, Misawa N, Sakuma T, Kobayashi T, Yamamoto T, Koyanagi Y	PLoS One	印刷中	国外
APOBEC3D and APOBEC3F potently promote HIV-1 diversification and evolution in humanized mouse model	Sato K, Takeuchi JS, Misawa N, Izumi T, Kobayashi T, Kimura Y, Iwami S, Takaori-Kondo A, Hu W-S, Aihara K, Ito M, An DS, Pathak VK, Koyanagi Y	PLoS Pathogens	2014 年 10 月	国外
ゲノム編集技術を用いたエイズ根治療法の可能性	蝦名博貴、小柳義夫	羊土社	2014 年 6 月	国内
HIV-1 のウイルス学	佐藤佳、小柳義夫	最新医学社	2014 年 12 月	国内
ゲノム編集とエイズ治療	蝦名博貴、小柳義夫	医歯薬出版株式会社	2015 年 1 月	国内
Distinct combinations of amino acid substitutions in N-terminal domain of Gag-capsid afford HIV-1 resistance to rhesus TRIM5 α .	Nomaguchi M, Nakayama EE, Yokoyama M, Doi N, Igarashi T, Shioda T, Sato H, Adachi A	Microbes and infection	2014 年 11 月	国外
Fluorescent image analysis of HIV-1 and HIV-2 uncoating kinetics in the presence of old world monkey TRIM5 α .	Takeda E, Kono K, Hulme AE, Hope TJ, Nakayama EE, Shioda T	PLoS One	印刷中	国外
The HIV-1 gp120/CXCR4 axis promotes CCR7 ligand-dependent CD4 T cell migration: CCR7 homo- and CCR7/CXCR4 hetero-oligomer formation as a possible mechanism for up-regulation of functional CCR7.	Hayasaka H, Kobayashi D, Yoshimura H, Nakayama EE, Shioda T, Miyasaka M	PLoS One	2015 年 2 月	国外
Development of T cell lymphoma in HTLV-1 bZIP factor and Tax double transgenic mice.	Zhao T, Satou Y, Matsuoka M	Arch Virol	2014 年 6 月	国外
Japanese Drug Resistance HIVSN: Phylodynamic analysis reveals CRF01_AE dissemination between Japan and neighboring Asian countries and the role of intravenous drug use in transmission	Shiino T, Hattori J, Yokomaku Y, Iwatani Y, Sugiura W	PLoS One	2014 年 6 月	国外
Sequence and structural determinants of human APOBEC3H deaminase and anti-HIV-1 activities	Mitra M, Singer D, Mano Y, Hritz J, Nam G, Gorelick RJ, Byeon IJ, Gronenborn AM, Iwatani Y, Levin JG	Retrovirology	2015 年 1 月	国外
APOBEC3H polymorphisms associated with the susceptibility to HIV-1 infection and AIDS progression in Japanese.	Sakurai D, Iwatani Y, Ohtani H, Naruse T, Terunuma H, Sugiura W, Kimura A	Immunogenetics	印刷中	国外

Structural basis of clade-specific HIV-1 neutralization by humanized anti-V3 monoclonal antibody KD-247.	Kirby KA, Ong YT, Hachiya A, Laughlin TG, Chiang LA, Pan Y, Moran JL, Marchand B, Singh K, Gallazzi F, Quinn TP, Yoshimura K, Murakami T, Matsushita S, Sarafianos SG	FASEB Journal	2015 年 1 月	国外
Impact of maraviroc-resistant and low-CCR5-adapted mutations induced by in vitro passage on sensitivity to anti-envelope neutralizing antibodies.	Yoshimura K, Harada S, Boonchawalit S, Kawanami Y, Matsushita S	JOURNAL OF GENERAL VIROLOGY	2014 年 5 月	国外
Passive transfer of neutralizing monoclonal antibody KD-247 reduces plasma viral load in patients chronically infected with HIV-1.	Matsushita S, Yoshimura K, Ramirez K-P, Pisupati J, Jenkins J, Murakami T on behalf of the KD-1002 Study Group	AIDS	2015 年 2 月	国外
Complementary and synergistic activities of anti-V3, CD4bs and CD4i antibodies derived from a single individual can cover a wide range of HIV-1 strains.	Ramirez K-P, Kuwata T, Maruta Y, Tanaka K, Alam M, Yoshimura K, Matsushita S	Virology	2015 年 1 月	国外

VI. 研究成果の刊行物・別刷

TCF1 and LEF1 act as T-cell intrinsic HTLV-1 antagonists by targeting Tax

Guangyong Ma[a], Jun-ichirou Yasunaga[a,1], Hirofumi Akari[b], and Masao Matsuoka[a,1]

[a]Laboratory of Virus Control, Institute for Virus Research, Kyoto University, Kyoto 606-8507, Japan; and [b]Center for Human Evolution Modeling Research, Primate Research Institute, Kyoto University, Inuyama, Aichi 484-8506, Japan

Edited by Patrick L. Green, The Ohio State University, Columbus, Ohio, and accepted by the Editorial Board January 12, 2015 (received for review October 5, 2014)

Human T-cell leukemia virus type 1 (HTLV-1) is a delta-type retrovirus that induces malignant and inflammatory diseases during its long persistence in vivo. HTLV-1 can infect various kinds of cells; however, HTLV-1 provirus is predominantly found in peripheral CD4 T cells in vivo. Here we find that TCF1 and LEF1, two Wnt transcription factors that are specifically expressed in T cells, inhibit viral replication through antagonizing Tax functions. TCF1 and LEF1 can each interact with Tax and inhibit Tax-dependent viral expression and activation of NF-κB and AP-1. As a result, HTLV-1 replication is suppressed in the presence of either TCF1 or LEF1. On the other hand, T-cell activation suppresses the expression of both TCF1 and LEF1, and this suppression enables Tax to function as an activator. We analyzed the thymus of a simian T-cell leukemia virus type 1 (STLV-1) infected Japanese macaque, and found a negative correlation between proviral load and TCF1/LEF1 expression in various T-cell subsets, supporting the idea that TCF1 and LEF1 negatively regulate HTLV-1 replication and the proliferation of infected cells. Thus, this study identified TCF1 and LEF1 as Tax antagonistic factors in vivo, a fact which may critically influence the peripheral T-cell tropism of this virus.

HTLV-1 | Tax | TCF1 | LEF1

Human T-cell leukemia virus type 1 (HTLV-1) causes a malignancy named adult T-cell leukemia (ATL) and several inflammatory diseases including HTLV-1–associated myelopathy/tropical spastic paraparesis (HAM/TSP) (1, 2). HTLV-1 encodes a critical transactivator, Tax, that induces the activation and subsequent clonal expansion of infected T cells in vivo (2, 3). Tax is transcribed from the viral promoter 5′ long terminal repeat (LTR), where it further enhances HTLV-1 viral transcription by recruiting cellular CREB protein to Tax-responsive elements (TRE). However, Tax expression is frequently silenced in ATL cells due to genetic and epigenetic changes in the viral 5′ LTR and the *tax* gene (4–7), a possible consequence of host immune surveillance (8). On the other hand, the viral 3′ LTR remains intact and is responsible for consistent expression of the HTLV-1 bZIP factor (HBZ), a negative strand encoded accessory gene, in all ATL cells (9).

T-cell factor 1 (TCF1) and lymphoid-enhancer binding factor 1 (LEF1) are transcription factors of the Wnt pathway that bind to β-catenin to coactivate the downstream cascade (10, 11). They are predominantly expressed in T-lineage cells, with immature thymocytes having the highest expression (12). Thymocyte development was impaired in TCF1 knockout mice (13). Although LEF1 knockout did not significantly affect T-cell development, deficiency in both TCF1 and LEF1 resulted in a complete block at the immature single positive stage, indicating a functional redundancy of TCF1/LEF1 and their indispensible role in driving T-cell development (14). In contrast, their functions in peripheral T cells remain poorly characterized although a quite different role has been suggested due to their reduced expression upon T-cell receptor (TCR) engagement in CD8 T cells (15).

HTLV-1 is peripheral mature T-cell tropic. However, the mechanism of this tropism remains to be elucidated. Here we find that TCF1 and LEF1 are T-cell intrinsic factors that suppress HTLV-1 replication via antagonizing Tax. They interact with Tax and suppress its transactivating abilities. As a result, viral transcription and replication are greatly suppressed by either TCF1 or LEF1, resulting in selective viral replication in TCF1/LEF1 low-expressing T cells. At the same time, Tax is able to down-regulate TCF1/LEF1 by inducing STAT5a expression. We further demonstrate that thymocytes from a simian T-cell leukemia virus type 1 (STLV-1) infected Japanese macaque have low viral abundance and low 5′ LTR activity, negatively correlating with their high expression of TCF1 and LEF1.

Results

TCF1/LEF1 Are Expressed at Low Levels in HTLV-1–Infected T Cells. Previously we reported that HBZ impaired the DNA-binding ability of TCF1/LEF1 and thereby suppressed the canonical Wnt pathway, shaping an HTLV-1 favorable host environment (16). Interestingly, upon further study, we found that TCF1 and LEF1 mRNA and protein levels were invariably low in HTLV-1–infected cell lines, in contrast to most HTLV-1–negative T-cell lines except Kit225 (Fig. 1 *A* and *B*). Fresh ATL cells exhibited reduced expression of TCF1 and LEF1 compared with CD4 T cells from a healthy donor (Fig. 1*C*). Moreover, by analyzing microarray data of HTLV-1–infected individuals including asymptomatic carriers (AC), HAM/TSP, and ATL patients (GSE19080 and GSE33615), we observed similar down-regulation of TCF1 and LEF1 (Fig. S1 *A* and *B*).

Significance

HTLV-1 is a peripheral T-cell tropic virus and induces proliferation of CD4+ T cells, resulting in T-cell malignancy and inflammatory diseases. Recent studies demonstrated that several restriction factors inhibiting HIV are also inhibitory to HTLV-1. We identified two T-cell–specific proteins, TCF1 and LEF1, as HTLV-1 restriction factors that determine the peripheral T-cell tropism of this virus by targeting Tax. They are highly expressed in immature thymocytes and thereby become a natural intrinsic barrier for HTLV-1 replication in the thymus. However, their expression can be down-regulated by Tax, as well as by activation and differentiation of T cells. These findings provide a mechanistic understanding of how HTLV-1 induces T-cell malignancies in the periphery but never in the thymus.

Author contributions: G.M., J.-i.Y., and M.M. designed research; G.M. and J.-i.Y. performed research; H.A. contributed new reagents/analytic tools; G.M., J.-i.Y., and M.M. analyzed data; G.M., J.-i.Y., and M.M. wrote the paper.

The authors declare no conflict of interest.

This article is a PNAS Direct Submission. P.L.G. is a guest editor invited by the Editorial Board.

[1]To whom correspondence may be addressed. Email: mmatsuok@virus.kyoto-u.ac.jp or jyasunag@virus.kyoto-u.ac.jp.

This article contains supporting information online at www.pnas.org/lookup/suppl/doi:10.1073/pnas.1419198112/-/DCSupplemental.

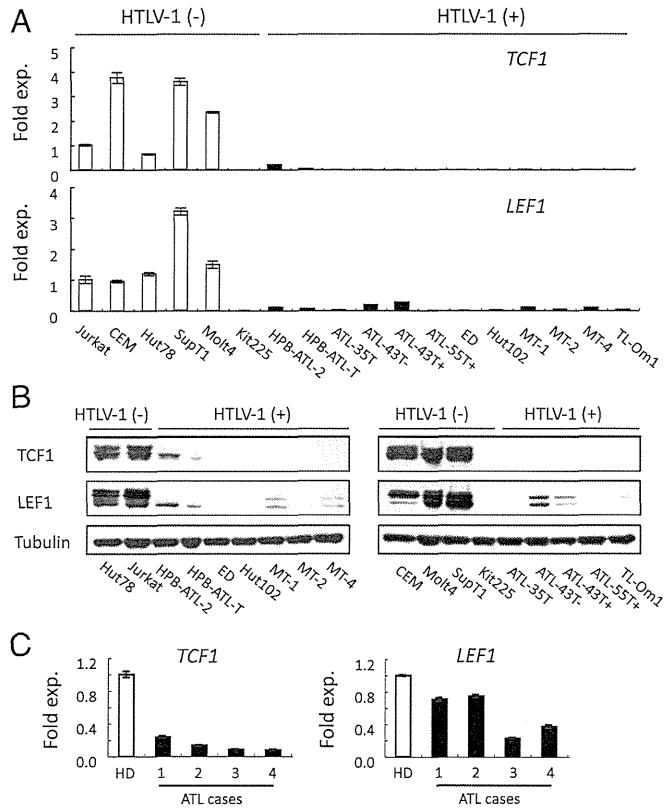

Fig. 1. TCF1 and LEF1 are expressed at low levels in HTLV-1–infected T cells. (*A*) TCF1 and LEF1 mRNA expression is invariably low in HTLV-1–infected cell lines. Total RNA was extracted for each cell line and subjected to quantitative real-time PCR (qPCR) analysis. Results are shown as relative mRNA expression of TCF1 or LEF1 normalized to that of 18S rRNA. (*B*) TCF1 and LEF1 protein expression of cell lines used in *A*. α-tubulin expression was used as a control. (*C*) TCF1 and LEF1 mRNA expression is lower in fresh ATL cases. Peripheral CD4 T cells from a healthy donor (HD) and four ATL patients were subjected to RNA extraction and following qPCR analysis. Results are shown as relative mRNA expression of TCF1 or LEF1 normalized to that of 18S rRNA. "Fold exp." indicates fold expression of normalized mRNA level of TCF1 or LEF1.

TCF1 and LEF1 Interact with Tax and Impair its Transactivating Ability. TCF family members have been recently reported to inhibit HIV type 1 (HIV-1) basal transcription (17). Therefore, we analyzed effects of TCF1 and LEF1 on transcription from the HTLV-1 LTR. As observed in HIV-1, we found that Tax-mediated activation of WT-Luc, which contains five tandem repeats of the TRE from HTLV-1 5′ LTR, was inhibited by TCF1 or LEF1 (Fig. 2*A*). Moreover, activation of the NFκB and AP1 pathways by Tax was also suppressed by TCF1 or LEF1 (Fig. 2*A*). Neither the activator of the Wnt pathway β-catenin nor the inhibitor Axin2 had such effects (Fig. S2*A*), indicating that the effects of TCF1 and LEF1 were mediated in a Wnt-independent manner. Furthermore, neither TCF1 nor LEF1 could inhibit the activation of these reporters by other transcription factors (Fig. S2*B*), suggesting that TCF1 and LEF1 specifically impair Tax function. We performed coimmunoprecipitation (co-IP) and found that TCF1 and LEF1 could each associate physically with Tax in vivo (Fig. 2*B*). Using a series of deletion mutants of Tax, we found that TCF1 and LEF1 predominantly bound to the C-terminal region of Tax (Fig. S2*C*). The PDZ-binding motif (PBM) is known to be localized in the C-terminal end of Tax (3). We found that removal of the PBM greatly impaired Tax binding to TCF1 or LEF1 (Fig. 2*C*), indicating that the PBM of Tax is critical for its binding with TCF1/LEF1. However, Tax bound to distinct regions of TCF1 and LEF1. The central regulation domain of TCF1 was indispensable for binding to Tax whereas all three domains were required for LEF1 to bind to Tax properly (Fig. S3*A*). Reporter assays with WT-Luc also functionally verified this result (Fig. S3*B*).

Nevertheless, due to their broad-spectrum antagonism of Tax, we suspected TCF1 and LEF1 might competitively bind to Tax over other host factors that are hijacked by Tax for transactivation of the viral LTR. CREB is recruited by Tax for its activation of the HTLV-1 5′ LTR (3). We found that TCF1 or LEF1 dose-dependently displaced CREB from Tax (Fig. 2*D*), which suggests that TCF1 and LEF1 each hinder the interaction between Tax and CREB. Thus, these data demonstrate that TCF1 and LEF1 are Tax antagonists that likely execute their inhibition via direct interaction with Tax.

TCF1 and LEF1 Inhibit HTLV-1 Replication by Antagonizing Tax. Next we examined the biological effects of this antagonism on Tax. HTLV-1 replication depends on Tax-driven transcription from the 5′ LTR. To address whether TCF1 and LEF1 are detrimental to HTLV-1 replication, we used an infectious clone of HTLV-1, pX1MT-M (18). HTLV-1 virus production measured by p19 ELISA was inhibited by TCF1 or LEF1 in a dose-dependent manner (Fig. 3*A*). Furthermore, expression of viral proteins that rely on Tax, such as gp46, p19, p24, and even Tax itself, was suppressed by TCF1 or LEF1 (Fig. 3*A*). We also found that endogenous TCF1 or LEF1 is also able to suppress HTLV-1 replication (Fig. S4).

On the other hand, HBZ transcription, which is initiated from viral 3′ LTR and slightly enhanced by Tax (19), was not suppressed but rather enhanced by TCF1 or LEF1 (Fig. 3*B*), in sharp contrast to Tax (Fig. 3*B*). To see whether this was associated with differential regulation of the HTLV-1 5′ and 3′ LTRs

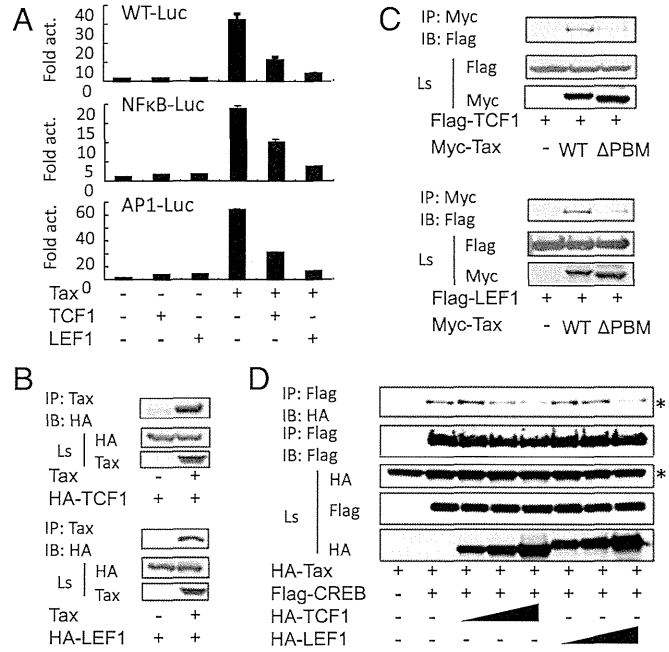

Fig. 2. TCF1 and LEF1 each interact with Tax and impair its transactivating ability. (*A*) TCF1 and LEF1 each repress Tax-mediated activation of WT-Luc (*Top*), NFκB-Luc (*Middle*), and AP1-Luc (*Bottom*). Reporter assays were performed in Jurkat cells. (*B*) Physical interactions between TCF1 and Tax (*Upper*), and LEF1 and Tax (*Lower*). (*C*) A ΔPBM mutant of Tax has impaired binding to TCF1 (*Upper*) and LEF1 (*Lower*) compared with WT Tax. (*D*) Physical interactions between Tax and CREB are inhibited by TCF1 or LEF1 in a dose-dependent manner. Tax-specific bands are denoted with an asterisk. All immunoprecipitations were performed in 293FT cells. "Ls" indicates the whole cell lysate.

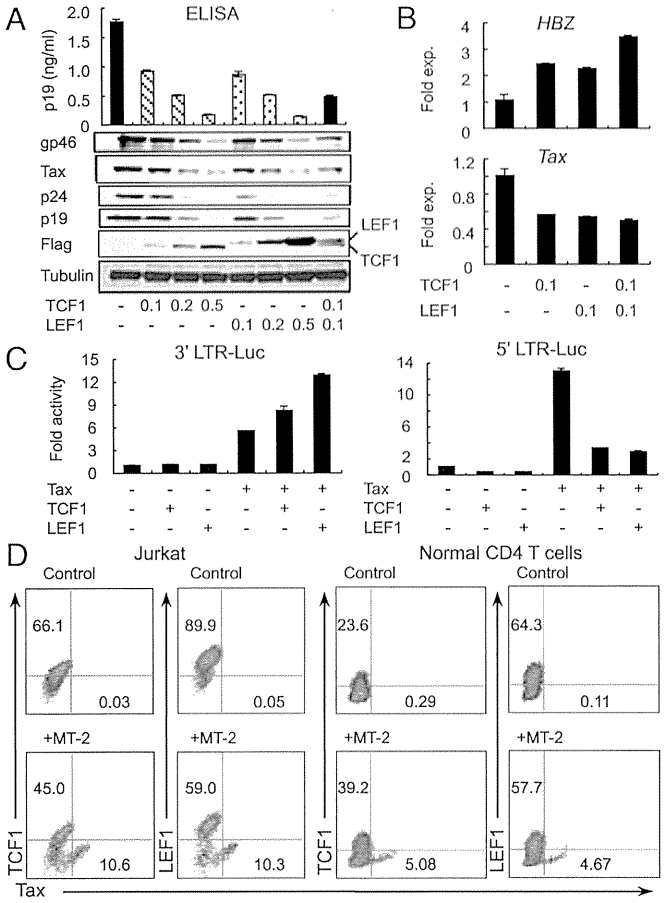

Fig. 3. TCF1 and LEF1 each inhibit HTLV-1 replication by antagonizing Tax. (*A*) TCF1 and LEF1 each inhibits HTLV-1 production (*Upper*) and protein expression (*Lower*). pX1MT-M (0.5 μg) was transfected with or without TCF1 or LEF1 into 293FT cells. 48 h later, supernatants were collected for p19 ELISA and cells were lysed for Western blot. (*B*) TCF1 and LEF1 each inhibit Tax transcription (*Lower*) but not HBZ transcription (*Upper*). pX1MT-M (0.5 μg) was transfected with or without TCF1 or LEF1 into 293FT cells. 44 h later, RNA was extracted for qPCR analysis. (*C*) TCF1 and LEF1 each slightly enhance Tax-mediated 3′ LTR-Luc (*Left*) activation, whereas they significantly suppress 5′ LTR activation (*Right*). Reporter assays were performed in Jurkat cells. (*D*) Jurkat or normal human CD4 T cells were either cultured alone (*Upper*) or cocultivated with lethally irradiated (150 Gy) MT-2 cells (*Lower*) at a 2:1 ratio. 48 h later (when MT-2 cells were all dead), cells were stained for intracellular Tax and TCF1 or LEF1. Numerals indicate percentages of gated populations. Fold exp. indicates fold expression.

by TCF1/LEF1, we performed reporter assays with the complete 5′ and 3′ LTR sequences. Tax mildly activated the 3′ LTR, and this activation was enhanced by TCF1 or LEF1 (Fig. 3*C*). This observation explains why HBZ transcription increased in the presence of TCF1/LEF1 (Fig. 3*B*). Consistent with the WT-Luc result (Fig. 2*A*), TCF1 or LEF1 significantly suppressed Tax-induced 5′ LTR activation (Fig. 3*C*). To evaluate the effect of TCF1/LEF1 upon HTLV-1 de novo infection, we cocultivated Jurkat or normal CD4 T cells with lethally irradiated MT-2 cells. Tax expression was detected predominantly in the TCF1/LEF1 low-expressing fraction (Fig. 3*D*), suggesting that TCF1/LEF1 restricts HTLV-1 de novo viral expression and its replication.

Tax Down-Regulates TCF1 and LEF1 via STAT5a. Antigen encounter or T-cell activation were reported to trigger TCF1/LEF1 down-regulation (15). We confirmed that phorbol myristate acetate (PMA)/ionomycin (P/I) stimulation down-regulate TCF1 and LEF1 in Jurkat and primary CD4 T cells (Fig. 4*A* and Fig. S5*A*). Therefore, we suspected that reduced expression of TCF1 and LEF1 in HTLV-1–infected cells is also caused by Tax, which is known to activate T cells (3). As expected, Tax induced the expression of the same activation markers as P/I stimulation (Fig. S5*B*), and suppressed the expression of TCF1 and LEF1 in Jurkat cells (Fig. 4*A*). Furthermore, cadmium-induced Tax expression in JPX-9, a modified Jurkat line that expresses Tax under a metallothionein promoter (20), also down-regulated TCF1 and LEF1 (Fig. 4*B*). However, Tax (Fig. S5*C*) did not inhibit transcription from the TCF1 and LEF1 promoters. To see whether the NFκB, NFAT, or AP1 pathways, the three major TCR downstream pathways, are involved in TCF1/LEF1 down-regulation (21), we activated them by electroporation of the corresponding transcription factors into Jurkat (Fig. S5*D*). However, neither single nor combined activation of these pathways clearly suppressed TCF1 or LEF1 expression (Fig. S5*E*). JAK/STAT signaling, a major cytokine pathway of T cells that becomes active following T-cell activation (22), has been found to be constitutively active in HTLV-1–infected T cells (23). Because STAT proteins are transcription factors that activate this pathway (24), we examined the effect of STAT5a, which is reported to be a target of Tax (25). First, we confirmed that STAT5a expression was induced upon P/I stimulation and Tax expression (Fig. 4*C*). Then we overexpressed either the wild type or the constitutively active form of STAT5a in Jurkat cells, and found significantly decreased expression of TCF1 and LEF1 (Fig. 4*D*).

Higher Expression of TCF1 and LEF1 Is Associated with Low STLV-1 Proviral Load in Vivo. The above results suggest that Tax function and HTLV-1 replication are impaired in TCF1/LEF1 high expressing cells, most likely in thymocytes that express higher levels of TCF1/LEF1. To analyze the relationship between TCF1/LEF1 expression and proviral load (PVL) in vivo, a model of HTLV-1 infection was required. We have reported that

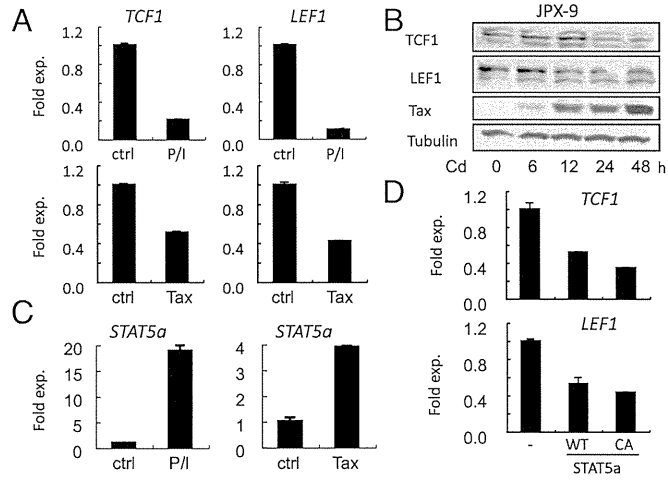

Fig. 4. Tax down-regulates the expression of TCF1 and LEF1 via STAT5a. (*A*) P/I stimulation (*Upper*) or Tax overexpression (*Lower*) inhibits TCF1/LEF1 transcription in Jurkat. For P/I stimulation, cells were treated with 50 ng/mL of PMA and 500 ng/mL of ionomycin (P/I) for 5 h and then subjected to RNA extraction and qPCR analysis. Overexpression of Tax was achieved by electroporation and 24 h later, RNA was extracted for qPCR. (*B*) Tax induction in JPX-9 down-regulates the expression of TCF1 and LEF1. JPX-9 was cultured in RPMI supplemented with 20 μM of cadmium (Cd) to induce Tax expression. At indicated time points, cells were lysed for Western blot analysis. (*C*) P/I stimulation or Tax overexpression induces STAT5a expression in Jurkat. P/I stimulation and Tax overexpression were performed as in *A*. (*D*) Overexpression of STAT5a down-regulates TCF1 and LEF1. Jurkat was transfected with wild type (WT) or constitutively active (CA) STAT5a by electroporation. 24 h later, RNA was extracted for qPCR. Fold exp. indicates fold expression.

STLV-1 encoded Tax and STLV-1 bZIP factor (SBZ) possess functions similar to those of HTLV-1 Tax and HBZ, and an STLV-1–infected Japanese macaque developed T-cell lymphoma (26), indicating that STLV-1–infected Japanese macaques can serve as a suitable model of HTLV-1 infection. STLV-1 Tax is highly homologous to HTLV-1 Tax (26). Similar to HTLV-1 Tax, it also has a typical PDZ-binding motif (ETDV) in its C-terminal end. We sorted various T-cell subsets from an STLV-1–infected Japanese macaque (Fig. S6) and found that CD4+CD8+ thymocytes (T-DP) showed the highest expression levels of TCF1 and LEF1 (Fig. 5*A*) whereas their PVL was the lowest (Fig. 5*B*). This result is consistent with our hypothesis that TCF1 and LEF1 inhibit viral expansion through impairing both the function and expression of Tax (Fig. 2 and 3). CD4+ thymocytes (T-CD4) were about twofold higher in TCF1/LEF1 expression (Fig. 5*A*) than their counterparts in the periphery (P-CD4). However, the PVL of P-CD4 T cells was 10-fold higher than that of T-CD4 T cells (Fig. 5*B*). Similar measurements were made in thymic (T-CD8) and peripheral CD8 T cells (P-CD8) (Fig. 5*A* and *B*). Interestingly, only a 1.3-fold increase of PVL in P-CD8 over T-CD8 was observed, in contrast to a 10-fold increase in P-CD4 over T-CD4 (Fig. 5*B*). Along with the fact that thymic CD8 and CD4 T cells had similar PVLs, this observation implies a much smaller expansion of infected CD8 T cells in the periphery than of CD4 T cells, an observation in agreement with a previous report showing that HTLV-1's in vivo tropism is a consequence of predominant expansion of peripheral CD4 over CD8 T cells (27).

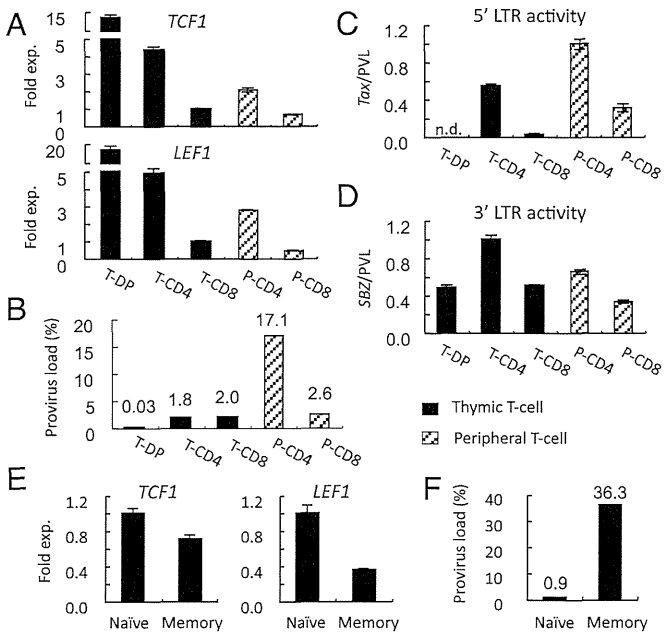

Fig. 5. TCF1 and LEF1 expression correlate negatively with STLV-1 proviral load in vivo. (*A*) TCF1 (*Upper*) and LEF1 (*Lower*) transcription in sorted CD4/CD8 double positive (T-DP), CD4 single positive (SP) thymocytes (T-CD4), CD8 SP thymocytes (T-CD8) and peripheral CD4 (P-CD4) and CD8 (P-CD8) SP T-cells from an STLV-1–infected Japanese macaque, determined by qPCR. (*B*) Genomic DNAs of sorted T cells were analyzed for STLV-1 proviral load. Numerals indicate number of virus copies in 100 cells. (*C*) Relative 5′ LTR activity of infected T cells. Tax mRNA expression was normalized to PVL of the same subset to represent relative transcription efficiency from 5′ LTR. (*D*) Relative 3′ LTR activity of infected T cells determined by normalizing SBZ mRNA expression to PVL. (*E*) TCF1 (*Left*) and LEF1 (*Right*) mRNA expression in sorted CD3+CD4+CD45RA+ (naive) and CD45RA- (memory) T cells from the STLV-1–infected Japanese macaque, determined by qPCR. Fold exp. indicates fold expression. (*F*) Genomic DNAs of naïve and memory T cells were analyzed for STLV-1 proviral load. Numerals indicate number of virus copies in 100 cells.

Next we compared the levels of transcriptional activity from the 5′ and 3′ LTRs of the provirus in STLV-1–infected cells. We did this by normalizing either Tax or SBZ transcription to PVL. Recall that TCF1/LEF1 regulate transcription of these genes in opposing manners (Fig. 3*B*). The 5′ LTR was clearly more active in peripheral CD4 or CD8 T cells than their thymic counterparts (Fig. 5*C*). In contrast, transcription from the 3′ LTR was more active in thymocytes, although the differences were not so big as with the 5′LTR (Fig. 5*D*). Memory (CD45RA-) CD4 T cells from the spleen of the STLV-1–infected Japanese macaque showed lower TCF1 and LEF1 expression but much higher PVL than naïve (CD45RA+) CD4 T cells (Fig. 5 *E* and *F*), which is in agreement with the fact that HTLV-1–infected cells have mostly a memory phenotype (28).

Discussion

During coevolution between virus and the host, host cells acquire many restriction factors that suppress viral replication (29, 30). HTLV-1 is derived from STLV-1 in monkeys, just like HIV-1 is derived from SIV. Many restriction factors have been reported for HIV-1 (31). However, restriction factors for HTLV-1 have not been studied extensively. It has been reported that APOBEC3G suppresses replication of HTLV-1 whereas Gag protein inhibits incorporation of APOBEC3G into the virion (32). Recently, SAMHD1 has been reported to suppress replication of HTLV-1 in monocytes (33). Tax is indispensable for HTLV-1 replication because expression of most viral genes, including all HTLV-1 structural genes, depends on transcription from the 5′ LTR that is activated by Tax. Moreover, Tax also plays a key role in dysregulating the cellular environment toward one which favors viral propagation, such by activation and transformation of an infected T cell (2). It is presumed that the T-cell tropism of HTLV-1 is more likely determined by postinfection events triggered by the virus because viral receptors are expressed in a wide variety of host cells (34). This study suggests that TCF1 and LEF1 are factors that restrict the tropism of this virus to peripheral T cells. In thymocytes expressing high levels of TCF1 and LEF1, these factors impair the functions of Tax, likely hindering not only viral replication but also the proliferation of the infected cells.

Restriction of tropism to peripheral T cells is likely a useful adaptation for HTLV-1. If HTLV-1 could replicate efficiently in the thymus, it might cause serious damage to the host immune system and thus the host. Furthermore, this virus is transmitted via breast-feeding or sexual transmission through infected T cells, so infected T cells must enter breast milk or semen. Most T cells in breast milk are peripheral T cells with an effector/memory phenotype (35). Restriction by TCF1/LEF1 would explain viral tropism to peripheral T cells and facilitate transmission of the virus.

Neoplasm of immature T cells has not been reported in HTLV-1–infected individuals. However, transgenic expression of Tax in the thymus induced immature T-cell lymphomas (36). These findings suggest that overexpression of Tax is oncogenic even for thymocytes, but that Tax expression or functions are normally impaired in the thymus of infected individuals. This study presents a mechanism for how thymocytes are relatively resistant to HTLV-1 infection and leukemogenesis in vivo, by identifying TCF1 and LEF1 as antagonists for Tax. We discovered an unexpected Wnt-independent role of TCF1 and LEF1 as Tax antagonists and demonstrated that this antagonism renders thymocytes less permissive for HTLV-1 replication compared with peripheral T cells.

The roles of TCF1/LEF1 have been well established in the thymus; they are indispensable in driving T-cell development (37). Nevertheless, their functions in the periphery remain

unknown. Recent studies showed that down-regulation of TCF1/LEF1 always occurs in activated or differentiated peripheral T cells (38). HTLV-1 may exploit this down-regulation to achieve its expansion, because down-regulation of TCF1/LEF1 allows Tax to execute its functions. A previous report also indicated that preactivated primary T cells are easier to transform by HTLV-1 (39). Down-regulation of TCF1/LEF1 upon T-cell activation/differentiation would allow Tax expression and subsequent HTLV-1 expansion.

Down-regulation of TCF1/LEF1 also occurs as T cells develop or differentiate, from DP to SP in the thymus (Fig. 5*A*), or from naïve to memory in the periphery (Fig. 5*E*). Therefore, our results also imply an interesting possibility that HTLV-1 might achieve its expansion as infected T cells differentiate or even by driving differentiation of infected T cells to reduce TCF1/LEF1 expression. Indeed, a recent report using humanized mice showed altered T-cell development upon HTLV-1 infection in that the mature SP population, instead of immature DN or DP, becomes dominant in the thymus (40). This finding suggests that thymocytes are propelled to develop by HTLV-1 or the virus selectively expands in the more differentiated subsets. Similarly, in a previous study of peripheral T cells, we demonstrated that HTLV-1–infected T cells were mostly memory cells and the number of naïve cells was significantly decreased (28). Our current results also reveal the preferential infection of CD4 effector/memory T cells by STLV-1. However, to clarify the roles of T-cell development/differentiation in contributions of HTLV-1 expansion, further studies are needed.

STLV-1–infected Japanese macaque has been demonstrated to be a suitable model for HTLV-1 infection (26). It also served as an ideal model to analyze the impact of the antagonism of TCF1/LEF1 against Tax in vivo. However, due to the complexity of viral infections in vivo, other factors such as the susceptibility to viral infections, postinfection mitotic potential and cytotoxic T-cell killing efficiency might affect the consequence of an infection in a specific T-cell subset. Indeed, the tropism of the virus for peripheral CD4 T cells over peripheral CD8 T cells does not appear to be explained by TCF1/LEF1 levels. More detailed investigations in STLV-1–infected Japanese macaques are expected to clarify these points in the future.

TCF1/LEF1 regulate the HTLV-1 5′ and 3′ LTR activities in opposing manners via their interplay with Tax (Fig. 3*C*). This may result in distinct expression levels of Tax and HBZ in vivo in different T-cell subsets or during various stages of infection. Interestingly, valproate, a histone deacetylase inhibitor, was reported to induce Tax expression while suppressing that of HBZ (41). These intriguing observations that the HTLV-1 5′ and 3′ LTR are regulated in opposite ways by multiple mechanisms, in addition to frequently observed contradictory functions of Tax and HBZ, may suggest a complex but fine-tuned viral pathogenesis. For instance, although activation of NF-κB pathway has been considered a critical function of Tax for cellular transformation (2, 3), the recent studies have reported that hyperactivation of NF-κB pathway induces cellular senescence whereas HBZ suppresses this action of Tax, thereby enabling clonal expansion (42). This study shows that TCF1/LEF1 inhibit Tax-mediated NF-κB activation by direct binding to Tax. Furthermore, TCF1/LEF1 inhibit various functions of Tax, whereas HBZ selectively modulates signaling pathways (43, 44). Thus, Tax and HBZ collaboratively function for clonal expansion and viral replication, whereas TCF1/LEF1 inhibit functions of Tax by direct interaction, which leads to suppression of viral replication and proliferation of infected cells.

In summary, we here identify TCF1 and LEF1 as previously unidentified Tax antagonists that likely restrict viral expansion in the thymus. The critical interplay of TCF1 and LEF1 with Tax during HTLV-1 infection may shed light on how HTLV-1 achieves its tropism and persistence in peripheral T cells in vivo.

Materials and Methods

Primary Samples Ethics Statement. The experiments using primary samples in this study were conducted according to the principles expressed in the Declaration of Helsinki. This study was approved by the Institutional Review Board of Kyoto University (approval numbers G310 and E2005). All ATL patients and healthy individuals provided written informed consent for the collection of samples and subsequent analysis. A Japanese macaque used in this study was 3 y old and naturally infected with STLV-1. The monkey was reared in the Primate Research Institute, Kyoto University. All animal studies were conducted in accordance with the protocols of experimental procedures approved by the Animal Welfare and Animal Care Committee of the Primate Research Institute (approval number 2011–095).

Cell Lines. ATL-derived T-cell lines (HPB-ATL-2, HPB-ATL-T, ATL-43T-, ATL-43T+, ATL-55T+, ED, MT-1, and TL-Om1), HTLV-1–transformed T-cell lines (ATL-35T, Hut102, MT-2, and MT-4) were used in this study. Jurkat, CEM, Hut78, SupT1, Molt4, and Kit225 are HTLV-1–negative T-cell lines. All T-cell lines were maintained in RPMI supplemented with 10% (vol/vol) FBS, whereas Kit225, ATL-43T+, and ATL-55T+ were maintained in the media supplemented with 100 U/mL of recombinant IL-2. 293FT (Life Technologies) is a subline of HEK293, which originated from a human embryonic kidney cell.

Plasmids. Expression vectors for TCF1, LEF1, and Tax were described (16, 45). Flag-CREB was made by subcloning the CREB coding sequence into pCAG-Flag. WT-Luc and 5′ LTR-Luc were kind gifts from J. Fujisawa, Kansai Medical University, Osaka. pX1MT-M was a generous gift from D. Derse, National Cancer Institute, Frederick, MD. NFκB-Luc and AP1-Luc were purchased from Stratagene. 3′ LTR-Luc was described (19).

Antibodies. Rabbit monoclonal antibodies for TCF1 (C63D9) and LEF1 (C12A5) were purchased from Cell Signaling Technology. HRP conjugated mouse anti-HA (12A5) antibody was purchased from Sigma. Mouse monoclonal antibodies against HTLV-1 gp46, p24, and p19 were purchased from Zeptometrix. Mouse monoclonal antibodies for FLAG (M2), Myc (9E10), α-tubulin (DM1A), and Tax (MI73) were described (16). For flow cytometric analysis of cell surface markers, APC-Cy7 anti-CD3 (SP34-2), PerCP-Cy5.5 anti-CD4 (OKT4), V500 anti-CD8 (RPA-T8), and PE anti-CD45RA (5H9) were used. PerCP-Cy5.5 anti-CD4 (OKT4) was purchased from Biolegend, whereas the others were from BD.

Detection of Tax and TCF1/LEF1 by Flow Cytometry. Intracellular staining for Tax and TCF1/LEF1 was performed using the kit from eBioscience. DyLight 649 conjugated donkey anti-rabbit IgG and FITC conjugated goat anti-mouse IgG were purchased from Biolegend. Normal mouse IgG was purchased from Santa Cruz and used for blocking nonspecific binding.

ELISA. Supernatants from cultured cells were centrifuged at 1,710 × *g* for 5 min to remove debris and then diluted and quantified for p19 by ELISA (Zeptometrix) according to manufacturer's instructions.

Sorting by FACS Aria II. See Fig. S6 for details.

Electroporation, real-time PCR, knockdown, Western blot, coimmunoprecipitation, and reporter assays were performed as described (16).

ACKNOWLEDGMENTS. We thank Drs. J. Fujisawa and D. Derse for providing reagents and Dr. L. Kingsbury for proofreading. We appreciate the help from Dr. Tani-ichi for cell sorting. This study was supported by a Grant-in-aid for Scientific Research on Innovative Area from the Ministry of Education, Science, Sports, and Culture of Japan (to M.M.) (22114003), and a grant from the Japan Leukemia Research Fund (to M.M.). This study was conducted by the Cooperation Research Program of the Primate Research Institute, Kyoto University.

1. Gallo RC (2005) History of the discoveries of the first human retroviruses: HTLV-1 and HTLV-2. *Oncogene* 24(39):5926–5930.
2. Matsuoka M, Jeang KT (2007) Human T-cell leukaemia virus type 1 (HTLV-1) infectivity and cellular transformation. *Nat Rev Cancer* 7(4):270–280.
3. Grassmann R, Aboud M, Jeang KT (2005) Molecular mechanisms of cellular transformation by HTLV-1 Tax. *Oncogene* 24(39):5976–5985.
4. Tamiya S, et al. (1996) Two types of defective human T-lymphotropic virus type I provirus in adult T-cell leukemia. *Blood* 88(8):3065–3073.

5. Takeda S, et al. (2004) Genetic and epigenetic inactivation of tax gene in adult T-cell leukemia cells. *Int J Cancer* 109(4):559–567.
6. Furukawa Y, Kubota R, Tara M, Izumo S, Osame M (2001) Existence of escape mutant in HTLV-I tax during the development of adult T-cell leukemia. *Blood* 97(4):987–993.
7. Koiwa T, et al. (2002) 5′-long terminal repeat-selective CpG methylation of latent human T-cell leukemia virus type 1 provirus in vitro and in vivo. *J Virol* 76(18): 9389–9397.
8. Bangham CR (2009) CTL quality and the control of human retroviral infections. *Eur J Immunol* 39(7):1700–1712.
9. Satou Y, Yasunaga J, Yoshida M, Matsuoka M (2006) HTLV-I basic leucine zipper factor gene mRNA supports proliferation of adult T cell leukemia cells. *Proc Natl Acad Sci USA* 103(3):720–725.
10. Staal FJ, Clevers HC (2005) WNT signalling and haematopoiesis: A WNT-WNT situation. *Nat Rev Immunol* 5(1):21–30.
11. Staal FJ, Luis TC, Tiemessen MM (2008) WNT signalling in the immune system: WNT is spreading its wings. *Nat Rev Immunol* 8(8):581–593.
12. Oosterwegel M, et al. (1993) Differential expression of the HMG box factors TCF-1 and LEF-1 during murine embryogenesis. *Development* 118(2):439–448.
13. Verbeek S, et al. (1995) An HMG-box-containing T-cell factor required for thymocyte differentiation. *Nature* 374(6517):70–74.
14. Okamura RM, et al. (1998) Redundant regulation of T cell differentiation and TCRalpha gene expression by the transcription factors LEF-1 and TCF-1. *Immunity* 8(1):11–20.
15. Willinger T, et al. (2006) Human naive CD8 T cells down-regulate expression of the WNT pathway transcription factors lymphoid enhancer binding factor 1 and transcription factor 7 (T cell factor-1) following antigen encounter in vitro and in vivo. *J Immunol* 176(3):1439–1446.
16. Ma G, Yasunaga J, Fan J, Yanagawa S, Matsuoka M (2013) HTLV-1 bZIP factor dysregulates the Wnt pathways to support proliferation and migration of adult T-cell leukemia cells. *Oncogene* 32(36):4222–4230.
17. Narasipura SD, et al. (2012) Role of β-catenin and TCF/LEF family members in transcriptional activity of HIV in astrocytes. *J Virol* 86(4):1911–1921.
18. Mitchell MS, et al. (2007) Phenotypic and genotypic comparisons of human T-cell leukemia virus type 1 reverse transcriptases from infected T-cell lines and patient samples. *J Virol* 81(9):4422–4428.
19. Yoshida M, Satou Y, Yasunaga J, Fujisawa J, Matsuoka M (2008) Transcriptional control of spliced and unspliced human T-cell leukemia virus type 1 bZIP factor (HBZ) gene. *J Virol* 82(19):9359–9368.
20. Azimi N, et al. (1998) Human T cell lymphotropic virus type I Tax protein trans-activates interleukin 15 gene transcription through an NF-kappaB site. *Proc Natl Acad Sci USA* 95(5):2452–2457.
21. Macian F (2005) NFAT proteins: Key regulators of T-cell development and function. *Nat Rev Immunol* 5(6):472–484.
22. Welte T, et al. (1999) STAT5 interaction with the T cell receptor complex and stimulation of T cell proliferation. *Science* 283(5399):222–225.
23. Migone TS, et al. (1995) Constitutively activated Jak-STAT pathway in T cells transformed with HTLV-I. *Science* 269(5220):79–81.
24. Lin JX, Leonard WJ (2000) The role of Stat5a and Stat5b in signaling by IL-2 family cytokines. *Oncogene* 19(21):2566–2576.
25. Nakamura N, et al. (1999) Human T-cell leukemia virus type 1 Tax protein induces the expression of STAT1 and STAT5 genes in T-cells. *Oncogene* 18(17):2667–2675.
26. Miura M, et al. (2013) Characterization of simian T-cell leukemia virus type 1 in naturally infected Japanese macaques as a model of HTLV-1 infection. *Retrovirology* 10:118.
27. Kannian P, et al. (2012) Distinct transformation tropism exhibited by human T lymphotropic virus type 1 (HTLV-1) and HTLV-2 is the result of postinfection T cell clonal expansion. *J Virol* 86(7):3757–3766.
28. Yasunaga Ji, et al. (2001) Impaired production of naive T lymphocytes in human T-cell leukemia virus type I-infected individuals: Its implications in the immunodeficient state. *Blood* 97(10):3177–3183.
29. Wolf D, Goff SP (2008) Host restriction factors blocking retroviral replication. *Annu Rev Genet* 42:143–163.
30. Bieniasz PD (2004) Intrinsic immunity: A front-line defense against viral attack. *Nat Immunol* 5(11):1109–1115.
31. Blanco-Melo D, Venkatesh S, Bieniasz PD (2012) Intrinsic cellular defenses against human immunodeficiency viruses. *Immunity* 37(3):399–411.
32. Derse D, Hill SA, Princler G, Lloyd P, Heidecker G (2007) Resistance of human T cell leukemia virus type 1 to APOBEC3G restriction is mediated by elements in nucleocapsid. *Proc Natl Acad Sci USA* 104(8):2915–2920.
33. Sze A, et al. (2013) Host restriction factor SAMHD1 limits human T cell leukemia virus type 1 infection of monocytes via STING-mediated apoptosis. *Cell Host Microbe* 14(4): 422–434.
34. Manel N, Battini JL, Taylor N, Sitbon M (2005) HTLV-1 tropism and envelope receptor. *Oncogene* 24(39):6016–6025.
35. Bertotto A, et al. (1990) Human breast milk T lymphocytes display the phenotype and functional characteristics of memory T cells. *Eur J Immunol* 20(8):1877–1880.
36. Hasegawa H, et al. (2006) Thymus-derived leukemia-lymphoma in mice transgenic for the Tax gene of human T-lymphotropic virus type I. *Nat Med* 12(4):466–472.
37. Weber BN, et al. (2011) A critical role for TCF-1 in T-lineage specification and differentiation. *Nature* 476(7358):63–68.
38. Xue HH, Zhao DM (2012) Regulation of mature T cell responses by the Wnt signaling pathway. *Ann N Y Acad Sci* 1247:16–33.
39. Merl S, et al. (1984) Efficient transformation of previously activated and dividing T lymphocytes by human T cell leukemia-lymphoma virus. *Blood* 64(5):967–974.
40. Villaudy J, et al. (2011) HTLV-1 propels thymic human T cell development in "human immune system" Rag2$^{-/-}$ gamma c$^{-/-}$ mice. *PLoS Pathog* 7(9):e1002231.
41. Belrose G, et al. (2011) Effects of valproate on Tax and HBZ expression in HTLV-1 and HAM/TSP T lymphocytes. *Blood* 118(9):2483–2491.
42. Zhi H, et al. (2011) NF-κB hyper-activation by HTLV-1 tax induces cellular senescence, but can be alleviated by the viral anti-sense protein HBZ. *PLoS Pathog* 7(4):e1002025.
43. Zhao T, et al. (2009) Human T-cell leukemia virus type 1 bZIP factor selectively suppresses the classical pathway of NF-kappaB. *Blood* 113(12):2755–2764.
44. Matsuoka M, Yasunaga J (2013) Human T-cell leukemia virus type 1: Replication, proliferation and propagation by Tax and HTLV-1 bZIP factor. *Curr Opin Virol* 3(6): 684–691.
45. Peloponese JM, Jr, Yasunaga J, Kinjo T, Watashi K, Jeang KT (2009) Peptidylproline cis-trans-isomerase Pin1 interacts with human T-cell leukemia virus type 1 tax and modulates its activation of NF-kappaB. *J Virol* 83(7):3238–3248.

PLOS | ONE

OPEN ACCESS

Citation: Fujie Y, Fusaki N, Katayama T, Hamasaki M, Soejima Y, et al. (2014) New Type of Sendai Virus Vector Provides Transgene-Free iPS Cells Derived from Chimpanzee Blood. PLoS ONE 9(12): e113052. doi:10.1371/journal.pone.0113052

Editor: Diego Fraidenraich, Rutgers University - New Jersey Medical School, United States of America

Received: July 15, 2014

Accepted: October 17, 2014

Published: December 5, 2014

Data Availability: The authors confirm that all data underlying the findings are fully available without restriction. All DNA array data can be found at the Gene Expression Omnibus (http://www.ncbi.nlm.nih.gov/geo/). The accession number is GSE 62572. Additional materials can be obtained by request from the corresponding author.

Funding: This study was supported in part by grants from the Ministry of Health, Labor, and Welfare of Japan, Precursory Research for Embryonic Science and Technology (PRESTO), and Core Research for Evolutional Science and Technology (CREST), Japan Science and Project of the Primate Research Institute, Kyoto University. DNAVEC Corporation provided support in the form of salaries for authors MH & HB, but did not have any additional role in the study design, data collection and analysis, decision to publish, or preparation of the manuscript. NF was provided with salary by JST grant (PRESTO). The specific roles of these authors are articulated in the 'author contributions' section.

Competing Interests: HB is an employee of DNAVEC Corporation. M. Hasegawa is a founder and adviser of DNAVEC Corporation. NF was an employee of DNAVEC Corporation until January 2013 but not now. The commercial product developed by DNAVEC Corporation is similar to the vectors described in this paper but the component is different. The patent of the Sendai virus vectors to generate iPS cells that was applied by and of DNAVEC Corporation is pending (WO/2010/008054). NF and HB have waived the right of the patent. These do not alter the authors'

RESEARCH ARTICLE

New Type of Sendai Virus Vector Provides Transgene-Free iPS Cells Derived from Chimpanzee Blood

Yasumitsu Fujie[1☯], Noemi Fusaki[2,3☯¤], Tomohiko Katayama[1], Makoto Hamasaki[1], Yumi Soejima[1], Minami Soga[1], Hiroshi Ban[2], Mamoru Hasegawa[2], Satoshi Yamashita[4], Shigemi Kimura[5], Saori Suzuki[6], Tetsuro Matsuzawa[7], Hirofumi Akari[6,8], Takumi Era[1]*

1. Department of Cell Modulation, Institute of Molecular Embryology and Genetics, Kumamoto University, 2-2-1 Honjo, Chuo-ku, Kumamoto 860-0811, Japan, **2.** DNAVEC Corporation, 6 Ookubo, Tsukuba, Ibaragi 300-2611, Japan, **3.** Precursory Research for Embryonic Science and Technology, Japan Science and Technology Agency, 4-1-8 Honcho Kawaguchi, Saitama, Japan, **4.** Department of Neurology, Graduate School of Medical Sciences, Kumamoto University, 1-1-1 Honjo, Chuo-ku, Kumamoto 860-8556, Japan, **5.** Department of Child Development, Graduate School of Medical Sciences, Kumamoto University, 1-1-1 Honjo, Chuo-ku, Kumamoto 860-8556, Japan, **6.** Section of Comparative Microbiology and Immunology, Center for Human Evolution Modeling Research, Primate Research Institute, Kyoto University, Inuyama, Aichi 484-8506, Japan, **7.** Section of Language and Intelligence, Primate Research Institute, Kyoto University, Inuyama, Aichi 484-8506, Japan, **8.** Laboratory of Evolutional Virology, Experimental Research Center for Infectious Diseases, Institute for Virus Research, Kyoto University, Kyoto, 606-8507, Japan

*tera@kumamoto-u.ac.jp

☯ These authors contributed equally to this work.

¤ Current address: Department of Ophthalmology, Keio University School of Medicine, 35 Shinano-machi, Shinjuku-ku, Tokyo 160-8582, Japan

Abstract

Induced pluripotent stem cells (iPSCs) are potentially valuable cell sources for disease models and future therapeutic applications; however, inefficient generation and the presence of integrated transgenes remain as problems limiting their current use. Here, we developed a new Sendai virus vector, TS12KOS, which has improved efficiency, does not integrate into the cellular DNA, and can be easily eliminated. TS12KOS carries *KLF4, OCT3/4*, and *SOX2* in a single vector and can easily generate iPSCs from human blood cells. Using TS12KOS, we established iPSC lines from chimpanzee blood, and used DNA array analysis to show that the global gene-expression pattern of chimpanzee iPSCs is similar to those of human embryonic stem cell and iPSC lines. These results demonstrated that our new vector is useful for generating iPSCs from the blood cells of both human and chimpanzee. In addition, the chimpanzee iPSCs are expected to facilitate unique studies into human physiology and disease.

adherence to all the PLOS ONE policies on sharing data and materials.

Introduction

Induced pluripotent stem cells (iPSCs) artificially produced from mammalian somatic cells including mouse and rat, human, marmoset, rhesus monkey, and pig can be induced to undergo sustained, unlimited growth and give rise to various cell types *in vitro* [1–7]. Because of these features, iPSCs have important potential applications as a source for cell therapy in clinical medicine. The iPSCs derived from patients also represent a powerful tool both for understanding disease pathogenesis and for investigating the effects of drugs at the individual and disease level on patient-derived cells [8].

While iPSCs derived from a range of mammalian species could serve as useful translational and disease models for cell and drug therapies, cell lines derived from nonhuman primates are particularly useful for such studies because the anatomical and physiological features of these species tend to be more similar to human than those of other mammals [9, 10]. Among nonhuman primates, the chimpanzee is often not a suitable experimental model because of breeding limitations; however, the chimpanzee shares some important physiological features with humans such as surface antigen cross-recognition by antibodies [11, 12]. Chimpanzees and humans occasionally share common pathogens, including ebola virus and hepatitis virus type B [13]. Thus, chimpanzee cells and stem cells derived from them represent powerful tools for both research and clinical applications in human disease.

The process of iPS cell generation, known as reprogramming, is triggered by the expression of four transcription factors, Oct3/4, Sox2, Klf4, and c-Myc, which are the same core factors underlying pluripotency in other stem cells such as embryonic stem cells (ESCs) [14]. Since overexpression of the four factors was initially mediated by lentivirus and retrovirus vectors in human skin-derived fibroblasts [5, 15], many methods have been reported including those involving transposons [16], proteins [17], microRNAs [18], and plasmids [19]. Recent progress has seen the increasing use of either plasmids or Sendai virus (SeV) vectors to generate iPS cells easily and quickly from human peripheral blood cells [20, 21]. Both methods are simple to conduct compared to other procedures, and are safer because there is no integration of transgenes into the host genome; however, the frequency of iPS cell colony generation remains low (~0.1%) and it is difficult to attain completely vector-free iPSCs.

Here, we generated a new SeV vector that enables highly efficient generation of iPS cells from peripheral blood cells, is temperature-sensitive (TS), and is quickly and efficiently eliminated from the established iPSCs by temperature shift. In addition to the generation of human iPSCs, we succeeded in establishing iPSC lines derived from the blood cells of chimpanzees.

Results

Vector generation

We previously generated iPSCs by using SeV vectors containing the sequences for four reprogramming factors (*OCT3/4*, *SOX2*, *KLF4* and *c-MYC*) [22]. Here, to increase the efficiency of iPSC generation and reduce the length of time the vector remains inside the cells, we generated a new TS-SeV vector, TS12KOS, carrying coding sequences for three of the above factors, *KLF4* (K), *OCT3/4* (O), and *SOX2* (S) (Fig. 1a) tandemly linked in the KOS direction. The TS12KOS vector contains three mutations that produce alanine residues (D433A, R434A, and K437A) in the large protein (L)-binding domain of the phosphoprotein (P), a component of SeV RNA polymerase. SeV carrying these three mutations showed moderate expression of GFP at 37℃, but weak expression at temperatures above 38℃ [23]. In a previous study, c-*MYC* was inserted between the sequences encoding the HN and L proteins in the TS15 SeV vector (HNL/TS15 c-MYC), which carries two other mutations (L1361C and L1558I) in addition to the triple mutation described above [23]. This vector is also temperature-sensitive and only weakly expressed at temperatures greater than 37℃. In this study, TS12KOS vector and a cocktail of conventional vectors carrying three reprogramming factors individually (*OCT3/4*, *SOX2* and *KLF4*), namely the conventional vectors, were used with HNL/TS15 c-MYC in following experiments.

First, we compared TS12KOS with the conventional SeV vectors for the efficiency of iPSC generation from human skin fibroblasts of healthy volunteers (Fig. 1b). Based on the numbers of colonies showing alkaline phosphatase (AP)-positive staining and human ESC-like morphology on day 28 after induction, we found that the efficiency of iPSC generation was significantly higher using the TS12KOS vector than with the conventional vectors.

We next examined the effect of temperature shift on iPSC generation from human fibroblasts. When the culture temperature was shifted from 37℃ to 36℃ for the initial two weeks after infection, the efficiency of colony formation remained high; however, when the temperature downshift continued for three weeks or more after infection, the efficiency tended to decrease in the samples from healthy volunteers (Fig. 1c). Therefore, a temperature downshift for the initial one week only was used in the following experiments.

We next conducted nested RT-PCR analysis of viral RNA to determine whether the TS12KOS vector was eliminated from the iPSCs earlier than the conventional SeV vectors. The nested RT-PCR analysis detects the viral genome with much higher sensitivity than single PCR [24]. We expanded the individual colonies and shifted the temperature from 37℃ to 38℃ for 3 days at various passages. In the conventional SeV infections, temperature upshifts at passage 1 or 2 induced no virus removal. In contrast, when the temperature of TS12KOS vector-infected cells was upshifted at passages 1 and 2, 84% and 65%, respectively, of iPSC-like clones were negative for viral genomic nucleic acid (Fig. 1d). These results indicated the TS12KOS vector superiority over the conventional SeV vectors in both efficiency of iPSC generation and elimination of virus from the iPSCs.

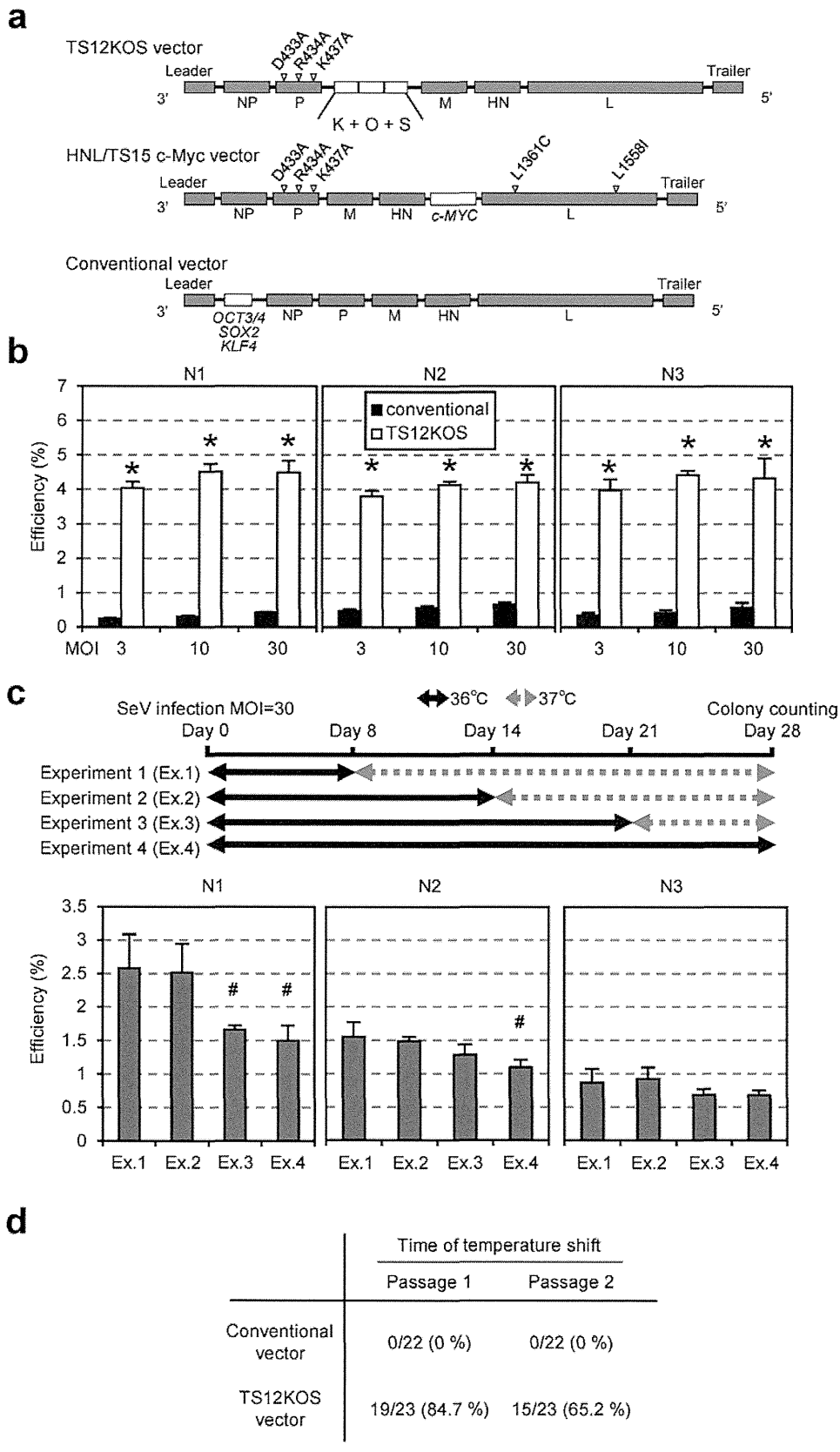
a
TS12KOS vector
Leader
D433A
R434A
K437A
Trailer
3'
NP
P
M
HN
L
5'
K + O + S
HNL/TS15 c-Myc vector
L1361C
L1558I
c-MYC
Conventional vector
OCT3/4
SOX2
KLF4
b
N1
N2
N3
conventional
TS12KOS
Efficiency (%)
MOI 3
10
30
c
SeV infection MOI=30
Day 0
36°C
37°C
Day 8
Day 14
Day 21
Colony counting
Day 28
Experiment 1 (Ex.1)
Experiment 2 (Ex.2)
Experiment 3 (Ex.3)
Experiment 4 (Ex.4)
Ex.1
Ex.2
Ex.3
Ex.4
d
Time of temperature shift
Passage 1
Passage 2
Conventional vector
0/22 (0 %)
0/22 (0 %)
TS12KOS vector
19/23 (84.7 %)
15/23 (65.2 %)

Figure 1. Generation of a new temperature-sensitive Sendai virus vector, TS12KOS. (**a**) Comparison of schematic structures among the newly constructed Sendai virus (SeV) vector, TS12KOS, and previous vectors. The TS12KOS vector contains three point mutations in the RNA polymerase–related gene (P) and carries the coding sequences of *KLF4* (K), *OCT3/4* (O), and *SOX2* (S) in the KOS direction. In comparison, the HNL/TS15 c-Myc vector carries two additional mutations, L1361C and L1558I, in the large polymerase (L) gene and an exogenous c-*MYC* cDNA sequence inserted between the hemagglutinin-neuraminidase (HN) and L genes, and the conventional vectors individually carry three reprogramming factors as indicated. (**b**) iPS cell generation from human skin-derived fibroblasts. The efficiency of iPS cell generation was significantly higher using the TS12KOS vector than with the conventional vectors at all multiplicities of infection (MOI) tested. iPSC colonies were identified on day 28 of induction by the appearance of alkaline phosphatase-positive (AP^+) colonies with embryonic stem (ES) cell-like colony morphology. N1, N2, and N3 represent individual healthy volunteers. Experiments were conducted in triplicate (mean ± SD). $^*P<0.01$, TS12KOS vector versus conventional vectors, Student's t-test. (**c**) Temperature shift from 37°C to 36°C for the indicated periods in iPSC generation. Data are means ± SD of three independent experiments. $^{\#}P<0.05$, Experiment 2, 3 and 4 versus Experiment 1. Student's t-test. (**d**) Nested RT-PCR analysis of SeV vector elimination after the temperature shift from 37°C to 38°C in human fibroblast-derived iPSCs. The elimination of TS12KOS vector was faster than the conventional vectors.

doi:10.1371/journal.pone.0113052.g001

Based on previous findings that L-*MYC* is safer than c-*MYC* due to a lower incidence of tumorigenicity, we next examined the effect of replacing the c-*MYC* cDNA sequences with L-*MYC* cDNA sequences in the HNL/TS15 c-MYC SeV vector (Fig. S1a) [25]. The frequency of colonies with ALP+ and ESC-like morphology was lower using the L-*MYC* vector than with the original HNL/TS15 c-MYC vector (Fig. S1b), despite the L-*MYC* gene showing higher expression levels (data not shown).

Because Glis1 can enhance iPSC generation, we also constructed and tested various SeV vectors carrying *GLIS1* sequences (Fig. S1a, c) [26]. Unexpectedly, Glis1 expression did not augment the colony formation from human skin-derived fibroblasts with or without c-Myc, suggesting that Glis1 does not play a part in iPSC induction with SeV vector (Fig. S1c).

Characterization of human iPS cells generated with new virus vector

Our ultimate goal is to develop safe and efficient vectors to generate iPSCs from both human and primate peripheral blood cells. When we stimulated human peripheral T lymphocytes with both anti-CD3 antibody and interleukin 2, and then infected them with SeV vectors, iPSC generation was significantly more efficient using the TS12KOS vector than with the conventional SeV vectors (Fig. 2a). In conventional SeV infections, temperature shifts from 37°C to 38°C at passages 1 and 2 induced no elimination of virus from the iPSC clones (Fig. 2b). In contrast, when TS12KOS vector was used under the same conditions, 65% and 47%, respectively, of the clones were negative for viral genome (Fig. 2b). Therefore, similar to the results obtained with fibroblasts, the elimination of TS12KOS vector from iPS-like cells derived from peripheral T lymphocytes was faster than that observed for the conventional SeV vectors.

The iPSC lines derived from skin fibroblasts and peripheral T lymphocytes induced by TS12KOS vector exhibited a typically ESC-like morphology and expressed a set of typical markers for pluripotency (Fig. 2c, d). These iPSC lines

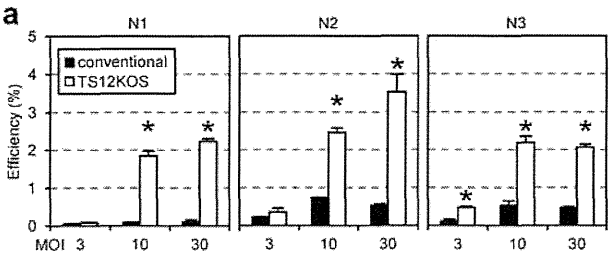

b

	Time of temperature shift	
	Passage 1	Passage 2
Conventional vector	0/18 (0 %)	0/18 (0 %)
TS12KOS vector	15/23 (65.2 %)	11/23 (47.8 %)

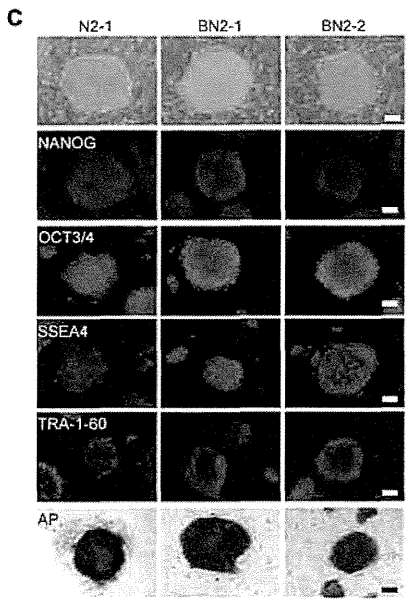

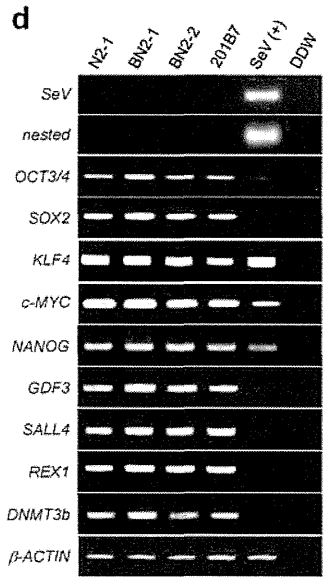

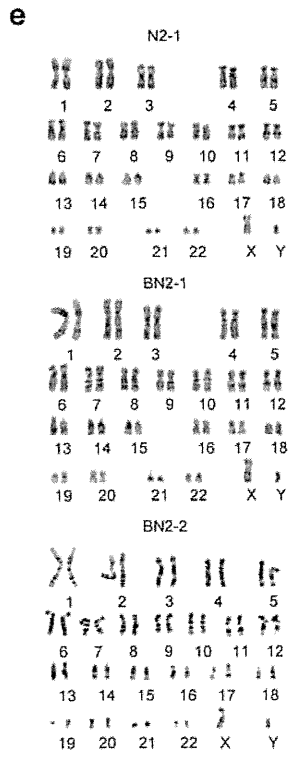

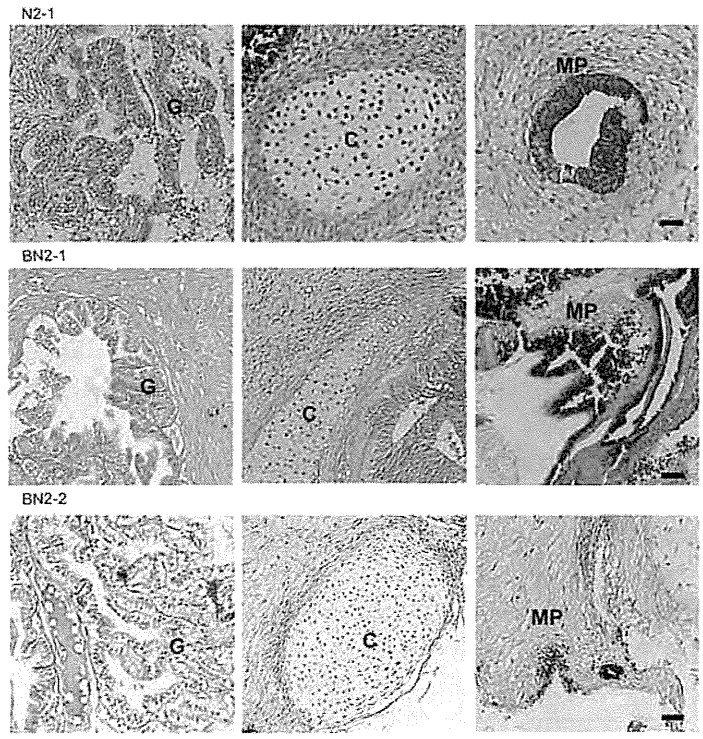

Figure 2. Characterization of human iPSCs generated by the TS12KOS vector. (**a**) iPSC generation from human peripheral blood cells. Experiments were conducted in triplicate (mean ± SD). N1, N2, and N3 indicate individual healthy volunteers. *$P<0.01$, TS12KOS vector versus conventional vectors, Student's t-test. (**b**) Nested RT-PCR analysis of the elimination of SeV vectors after the temperature shift from 37°C to 38°C. (**c**) Phase contrast images, immunofluorescence for pluripotency markers, and alkaline phosphatase (AP) staining of iPSC lines. The iPSC lines N2-1 and BN2-1 and BN2-2 were derived from the skin-derived fibroblasts and blood cells of N2 healthy volunteer, respectively. Scale bars, 200 μm. (**d**) RT-PCR analysis of Sendai virus and human ES cell markers. SeV, first RT-PCR for SeV; nested, nested RT-PCR for SeV; 201B7, control human iPSC line; SeV(+), Day 7 SeV-infected human fibroblasts. (**e**) Chromosomal analyses of iPSC lines generated with the TS12KOS vector. (**f**) Tissue morphology of a representative teratoma derived from iPSC lines generated with the TS12KOS vector. G, glandular structure (endoderm); C, cartilage (mesoderm); MP, melanin pigment (ectoderm). Scale bars, 100 μm.

doi:10.1371/journal.pone.0113052.g002

had a normal 46 XY karyotype even after the temperature upshift and culturing for more than 10 passages (Fig. 2e). To confirm the pluripotency of the clonal lines, we transplanted the lines into the testis of immunodeficient mice. Twelve weeks after injection, the iPSC lines tested formed teratomas that contained derivatives of all three germ layers (Fig. 2f). Based on these findings, we conclude that the iPSC lines generated with TS12KOS vector meet the criteria of iPSCs.

Establishment of chimpanzee iPS cells

Next we used the TS12KOS vector to establish iPSC lines from the blood cells of two chimpanzee individuals, with the ultimate goal of overcoming the limited availability of chimpanzee skin-fibroblasts for human medical use. Using the same protocol as for human blood cells, we could establish chimpanzee blood cell-derived iPSCs (Fig. 3a). However, the frequency was relatively low and only one cell line that carries the normal karyotype could be established (Experiment 1 in Fig. 3a). To optimize the induction conditions, we conducted *in vitro* human T lymphocyte stimulations with anti-CD3, Phytohaemagglutinin (PHA), or Concanavalin A (Con A), and similarly generated iPSCs from human peripheral mononuclear cells (PMNCs) using all three agents, with PHA stimulation the most efficient (Fig. 3b). The morphology of iPSC colonies derived from the anti-CD3- and PHA-stimulated PMNCs was distinct from colonies derived from the Con A-stimulated PMNCs (Fig 3c), which produced flat colonies with clearer and sharper edges than those derived from CD3- and PHA-stimulated PMNCs. In addition, many of the iPSC colonies derived from CD3- and PHA-stimulated PMNCs contained AP^+ cells in the center only (Fig. 3c). Together, these results suggested that colonies derived from Con A-stimulated PMNCs most closely fulfill the accepted criteria of iPSCs. Therefore, Con A was used in the following experiment 2 and 3 (Fig. 3a).

In addition, we changed the virus titer for infection from MOI 10 to 30 and the fibroblast growth factor 2 (FGF2) concentration from 5 ng/ml to 30 ng/ml during the iPSC induction (Fig. S2). The FGF2 change was based on a study of common marmosets, another nonhuman primate, which used 20 ng/ml FGF2 and treated the cultures with sodium butyrate (NaB) during reprogramming to enhance the iPSC colony number [7, 27]. In human blood cells, the efficiency of iPSC generation with 30 ng/ml FGF2 is slightly but not significantly lower than that with 5 ng/ml FGF2 (Fig. S3). Interestingly, these modifications improved the

a

	Chimpanzee No	Age	Sex	Stimulation Factor	SeV	MOI	FGF2 (ng/ml)	Frequency average(%)	Picked up Colonies	SeV(-) Colonies	Efficiency average(%)	Karyotype Normal No/Total No	Clone Name
Experiment 1	1	36	Female	anti-CD3 Ab	New	10	5	0.0016	2	2	100	1/2	C101
Experiment 2	2	46	Female	ConA	New	30	30	0.32	29	17	58.62	2/3	C201 C205
Experiment 3				ConA	Conv	30	30	0.073	11	2	18.18	1/2	C402